Chapter 16

Supersonic Flow

Version 0016.2k 11 February 2000

16.1 Overview

So far, we have mainly been concerned with flows that are slow enough that they may be treated as incompressible. We now consider flows in which the velocity approaches or even exceeds the speed of sound and in which density changes along streamlines cannot be ignored. Such flows are common in aeronautics and astrophysics. For example, the motion of a rocket through the atmosphere is faster than the speed of sound in air. In other words, it is *supersonic*. Therefore, if we transform into the frame of the rocket, the flow of air past the rocket is also supersonic.

When the flow speed exceeds the speed of sound in some reference frame, it is not possible for a pressure pulse to travel upstream in that frame and change the direction of the flow. However, if there is a solid body in the way (e.g. a rocket or aircraft), the flow direction must change. In a supersonic flow, this change happens nearly discontinuously, through the formation of *shock fronts* at which the flow suddenly decelerates from supersonic to subsonic. An example is shown in Fig. 16.1. Shock fronts are an inevitable feature of supersonic flows.

In another example of supersonic flow, a rocket itself is propelled by the thrust created by escaping hot gases from its exhaust. These hot gases move through the exhaust at supersonic speeds, expanding and cooling as they accelerate. In this manner the random thermal motion of the gas molecules is converted into an organised bulk motion that carries away negative momentum from the rocket and pushes it forward.

The solar wind furnishes yet another example of a supersonic flow. This high speed flow of ionized gas is accelerated in the solar corona and removes a fraction $\sim 10^{-14}$ of the sun's mass every year. Its own pressure accelerates it to supersonic speeds of ~ 400 km s^{-1}. When the outflowing solar wind encounters a planet, it is rapidly decelerated to a subsonic speed by passing through a strong discontinuity known as a *bow shock*, which surrounds the planet (Fig. 16.2). The bulk kinetic energy in the solar wind, built up during acceleration, is rapidly and irreversibly transformed into heat as it passes through this shock front.

In this chapter, we shall study some properties of supersonic flows. After restating the basic equations of compressible fluid dynamics (Sec. 16.2), we shall analyze three impor-

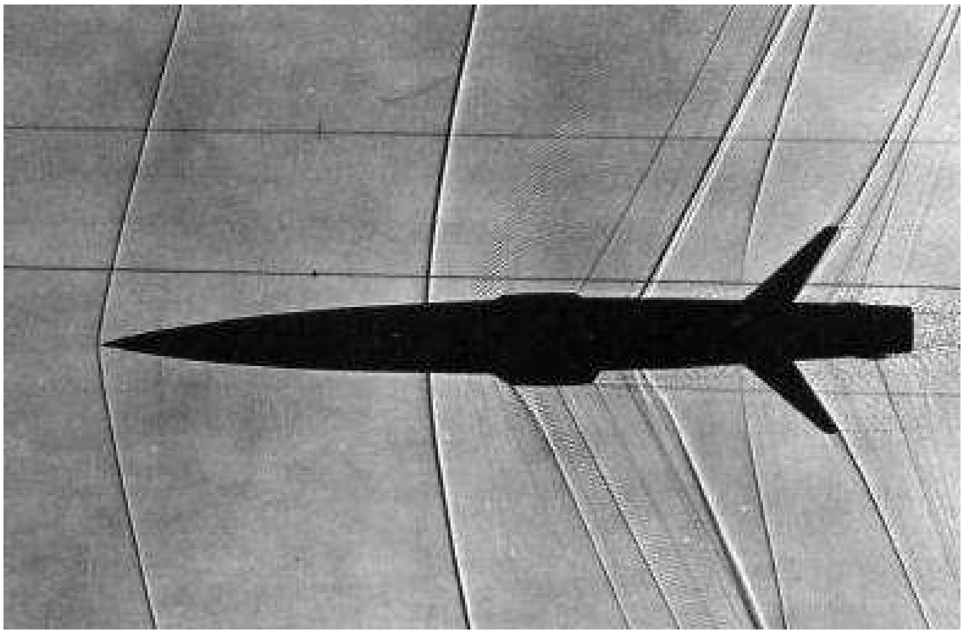

Fig. 16.1: Complex pattern of shock waves formed around a model aircraft in a wind tunnel with air moving ten percent facter than the speed of sound (i.e. with Mach number $M = 1.1$. Image from W. G. Vicenti, reproduced from Van Dyke 1982.)

tant, simple cases: quasi-one-dimensional stationary flow (Sec. 16.3), time-dependent one dimensional flow (Sec. 16.4), and normal adiabatic shock fronts (Sec. 16.5). In these sections, we shall apply the results of our analyses to some contemporary examples, including the Space Shuttle (Box 16.1), rocket engines, shock tubes, and the mach cone, N-wave and sonic booms produced by supersonic projectiles and aircraft. In Sec. 16.6, we will develop similarity-solution techniques for supersonic flows and apply them to supernovae, underwater depth charges, and nuclear-bomb explosions in the earth's atmosphere.

16.2 Equations of Compressible Flow

In Chap. 12, we derived the equations of fluid dynamics, allowing for compressibility. We expressed them as conservation laws for mass [Eq. (12.23)], momentum [Eq. (12.59)] and energy [Eq. (12.64) with vanishing right-hand side by virtue of (12.65)], and an evolution law for entropy [Eq. (12.67)]:

$$\frac{\partial \rho}{\partial t} + \nabla \cdot (\rho \mathbf{v}) = 0 \ , \tag{16.1}$$

$$\frac{\partial (\rho \mathbf{v})}{\partial t} + \nabla \cdot (P\mathbf{g} + \rho \mathbf{v} \otimes \mathbf{v} - 2\eta \boldsymbol{\sigma} - \zeta \theta \mathbf{g}) = \rho \mathbf{g}_e \ , \tag{16.2}$$

$$\frac{\partial}{\partial t}\left[(\frac{1}{2}v^2 + u + \phi)\rho\right] + \boldsymbol{\nabla} \cdot [(\frac{1}{2}v^2 + h + \phi)\rho \mathbf{v} - 2\eta \boldsymbol{\sigma} \cdot \mathbf{v} - \zeta \theta \mathbf{v}] = 0 \ , \tag{16.3}$$

$$\frac{\partial (\rho s)}{\partial t} + \boldsymbol{\nabla} \cdot (\rho s \mathbf{v}) = \frac{2\eta \boldsymbol{\sigma} : \boldsymbol{\sigma} + \zeta \theta^2}{T} \ . \tag{16.4}$$

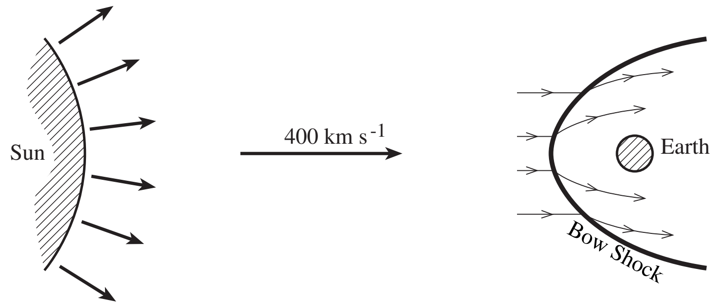

Fig. 16.2: The supersonic solar wind forms a type of shock front known as a bow shock when it passes by a planet.

Some comments are in order. Equation (16.1) is the complete mass conservation equation (continuity equation) assuming that matter is neither added to nor removed from the flow. Equation (16.2) expresses the conservation of momentum allowing for one external force, gravity. Other external forces can be added. Equation (16.3), expressing energy conservation, includes a viscous contribution to the energy flux. If there are sources or sinks of fluid energy, then these must be included on the right-hand side of this equation. Possible sources of energy include chemical or nuclear reactions; possible energy sinks include radiative cooling. We will incorporate the effects of heat conduction into the energy equation in the next chapter. Equation (16.4) expresses the evolution of entropy, and will also need modification if there are additional contributions to the energy equation. The right-hand side of this equation is the rate of increase of entropy due to viscous heating. This equation is not independent of the preceding equations and the laws of thermodynamics, but is often more convenient to use. In particular, one often uses it (together with the first law of thermodynamics) in place of the energy equation (16.3).

These equations must be supplemented with an equation of state in the form $P(\rho, T)$ or $P(\rho, s)$. For simplicity, we shall often focus on a perfect gas that undergoes adiabatic evolution with constant specific-heat ratio γ, so the equation of state has the simple form

$$P = K(s)\rho^\gamma \; . \tag{16.5}$$

Here $K(s)$ is a constant that depends on the entropy per unit mass s and is thus constant during the adiabatic evolution, but will change across shocks because the entropy increases in a shock (Sec. 16.5). For such a gas, we can integrate the first law of thermodynamics (Box 12.1) to obtain a formula for the internal energy per unit mass,

$$u = \frac{P}{(\gamma - 1)\rho} \; , \tag{16.6}$$

where we have assumed that the internal energy vanishes as the temperature $T \to 0$. It will prove convenient to express the density ρ, the internal energy per unit mass u and the enthalpy per unit mass h in terms of the sound speed

$$c = \sqrt{\left(\frac{\partial P}{\partial \rho}\right)_s} = \sqrt{\frac{\gamma P}{\rho}} \tag{16.7}$$

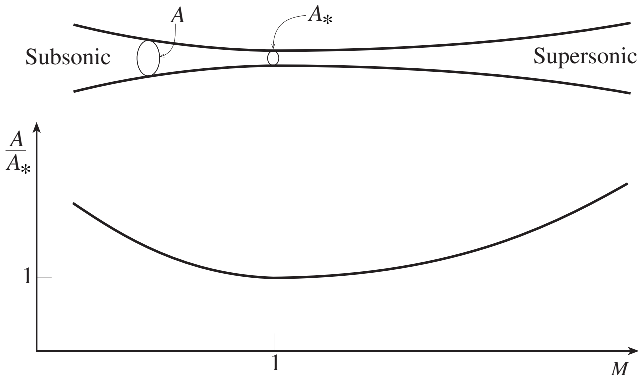

Fig. 16.3: Variation of cross sectional area, A, of a narrow bundle of flow lines as the Mach number, M, increases. Note that the flow is transonic ($M = 1$) when A is at its minimum, A_* .

[Eq. (15.69)]. A little algebra gives

$$\begin{aligned} \rho &= \left(\frac{c^2}{\gamma K}\right)^{1/(\gamma-1)} , \\ u &= \frac{c^2}{\gamma(\gamma-1)} , \\ h &= u + \frac{P}{\rho} = \frac{c^2}{\gamma - 1} . \end{aligned} \tag{16.8}$$

16.3 Stationary, Irrotational Flow

16.3.1 Quasi-One Dimensional Flow

In their full generality, the fluid dynamics equations (16.1)–(16.4) are quite unwieldy. In order to demonstrate some of the novel features of supersonic flow, we shall proceed as in earlier chapters: We shall specialize to a very simple type of flow in which the physical effects of interest are strong and extraneous effects are neglible. For supersonic flow this means a stationary ($\partial/\partial t = 0$), irrotational ($\boldsymbol{\nabla} \times \mathbf{v} = 0$) flow in which gravity and viscosity are negligible ($\Phi = \eta = \zeta = 0$), as are various effects not included in our general equations: chemical reactions, thermal conductivity and radiative losses. The vanishing viscosity implies [from the entropy evolution equation (16.4)] that the entropy per baryon s is constant along each flow line. We shall assume that s is the same on all flow lines, so the flow is fully isentropic (s constant everywhere) and the pressure $P = P(\rho, s)$ is thus a function only of the density, $P = P(\rho)$. When we need a specific form for $P(\rho)$, we will use that of an ideal gas with constant specific-heat ratio [Eqs. 16.5)–(16.8)], but much of our analysis will be done for a general isentropic $P(\rho)$. We will make one further approximation, that the flow is almost one dimensional. In other words, the velocity vectors all make small angles with each other in the region of interest.

These drastic simplifications are actually appropriate for many cases of practical interest! Granted these simplifications, we can consider a narrow bundle of streamlines which we call a *streamtube* and introduce, as a tool in studying it, its cross sectional area A, normal to the flow (Fig. 16.3).

As the flow is stationary, the equation of mass conservation (16.1) states that the rate at which mass passes through the streamtube's cross section must be independent of position along the tube:

$$\rho v A = \text{constant}; \tag{16.9}$$

here v is the speed of the fluid in the streamtube. Rewriting this in differential form, we obtain

$$\frac{dA}{A} + \frac{d\rho}{\rho} + \frac{dv}{v} = 0\ . \tag{16.10}$$

Because the flow is stationary and inviscid, the law of energy conservation (16.3) reduces to Bernoulli's theorem [Eqs. (12.39), (12.40)]:

$$\frac{1}{2}v^2 + h = \text{constant} \tag{16.11}$$

along each streamline and thus along our streamtube. Since the flow is adiabatic, we can use the first law of thermodynamics (Box 12.1) $dh = dP/\rho + Tds = dP/\rho = c^2 d\rho/\rho$ [where c is the speed of sound (16.7)] to write Eq. (16.11) in the differential form

$$\frac{d\rho}{\rho} + \frac{vdv}{c^2} = 0\ . \tag{16.12}$$

Finally and most importantly, we combine Eqs. (16.10) and (16.12) to obtain

$$\begin{aligned} \frac{d\ln A}{d\ln v} &= (M^2 - 1)\ , \\ \frac{d\ln A}{d\ln \rho} &= (M^{-2} - 1)\ , \end{aligned} \tag{16.13}$$

where

$$M \equiv v/c \tag{16.14}$$

is the *Mach number*. This Mach number is an important new dimensionless number that can be used to characterize compressible flows. When the Mach number is less than 1, the flow is called *subsonic*; when $M > 1$, it is *supersonic*. By contrast with the Reynolds, Rossby and Eckman numbers, which are usually defined using a single set of (characteristic) values of the flow parameters (V, ν, Ω, L) and thus have a single value for any given flow, the Mach number by convention is defined at each point in the flow and thus is a flow variable $M(\mathbf{x})$ similar to $v(\mathbf{x})$ and $\rho(\mathbf{x})$.

Equations (16.13) make remarkable predictions: At points along a streamtube where the flow is extremely subsonic $M \ll 1$, v varies inversely with A, in accord with everyday experience. At points where the flow is subsonic $M < 1$ but not extremely so, a decrease in the cross sectional area A still causes the fluid to speed up (v to increase), but not so strongly as when $M \ll 1$. By contrast, at points where the flow is supersonic $M > 1$, a

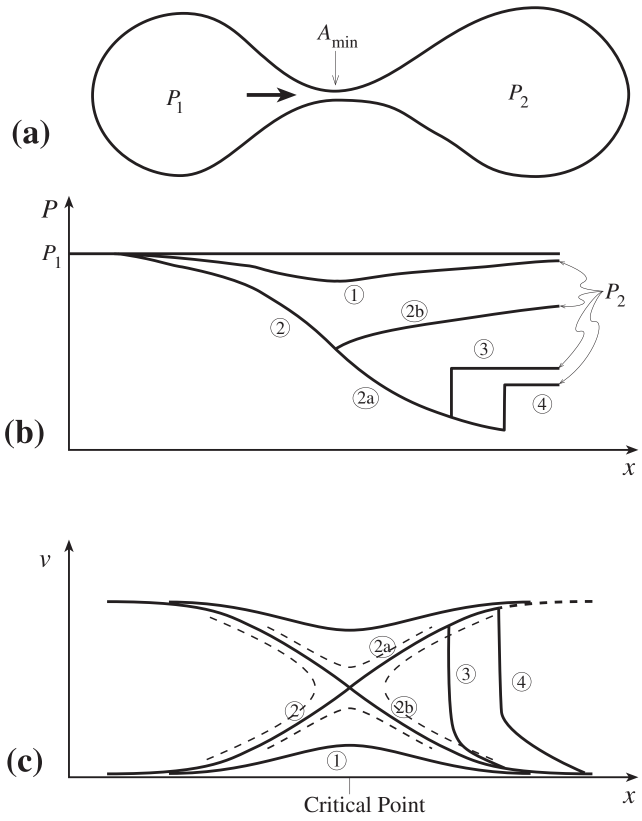

Fig. 16.4: Stationary flow through a channel between two chambers maintained at different pressures P_1 and P_2. When the pressure difference $P_1 - P_2$ is large enough, the flow is subsonic to the left of the channel's throat and supersonic to the right. As it nears or enters the second chamber, the supersonic flow must decelerate abruptly to a subsonic speed in a strong shock.

decrease of A causes the speed v to decrease, and an increase of A causes it to increase—just opposite to everyday, subsonic experience! However, mass is still conserved, $\rho v A =$ constant; the synchronous decrease (or increase) of v and A is compensated by the opposite evolution of ρ. At points where the flow is extremely supersonic $M \gg 1$, v remains nearly constant as A changes. Finally, a transition from subsonic to supersonic flow (i.e., a "transonic point" $M = 1$) can occur only at a minimum of the tube's area A. These conclusions are very useful in analyzing stationary, high-speed flows.

16.3.2 Setting up a Stationary, Transonic Flow

The reader may wonder, at this point, whether it is easy to set up a flow in which the speed of the fluid changes continuously from subsonic to supersonic. The answer is quite illuminating. We can illustrate the answer using two chambers maintained at different pressures, P_1 and P_2, and connected through a narrow channel along which the cross sectional area passes smoothly through a minimum $A = A_*$, the channel's *throat* (Fig. 16.4). When $P_2 = P_1$, there will be no flow between the two chambers. When we decrease P_2 slightly below P_1, there will be a slow subsonic flow through the channel (curve 1 in Fig. 16.4) that eventually will equalize the pressures. As we decrease P_2 further, there comes a point ($P = P_2^{\rm crit}$; curve 2) at which the flow is forced to be transonic at the channel's throat $A = A_*$. For all pressures $P_2 > P_2^{\rm crit}$, the flow is also transonic at the throat and has a universal form to the left of and near the throat, independent of the value of P_2—including a universal value for the rate of mass flow through the throat! This universal flow is supersonic to the right of the throat, but it *must* be brought to rest in chamber 2, since there is a hard wall at the chamber's end. How is it brought to rest? Through a shock front, where it is driven subsonic almost discontinuously (Sec. 16.5 below).

How, physically, is it possible for the flow to have a universal form to the left of the shock? The key to this is that in any supersonic region of the flow, disturbances are unable to propagate upstream, so the upstream fluid has no way of knowing what the pressure P_2 is in chamber 2. Although the flow to the left of the shock is universal, the location of the shock and the nature of the subsonic, post-shock flow *are* affected by P_2, since information can propagate upstream through that subsonic flow, from chamber 2 to the shock.

The reader might now begin to suspect that the throat, in the transonic case, is a very special location. It is, and that location is known as a *critical point* of the stationary flow. From a mathematical point of view, critical points are singular points of the equations of stationary flow [Eqs. (16.9)–(16.13)]. This singularity shows up in the solutions to the equations, as depicted in Fig. 16.4(c). The universal solution that passes transonically through the critical point (solution 2) joins onto two different solutions to the right of the throat: solution 2a, which is supersonic, and solution 2b, which is subsonic. Which solution occurs in practice depends on conditions downstream. Other solutions that are arbitrarily near this universal solution [dashed curves in Fig. 16.4(c)] are either double valued and consequently unphysical, or are everywhere subsonic or everywhere supersonic (in the absence of shocks).

The existence of critical points is a price we must pay, mathematically, for not allowing our equations to be time dependent. If we were to solve the time-dependent equations (which would then be partial differential equations), we would find that they change from elliptic to hyperbolic as the flow passes through a critical point.

From a physical point of view, critical points are the places where a sound wave propagating upstream remains at rest in the flow. They are therefore the one type of place from which time-dependent transients, associated with setting up the flow in the first place, cannot decay away (if the equations are dissipation-free, i.e., inviscid). Thus, even the time-dependent equations can display peculiar behaviors at a critical point. However, when dissipation is introduced, these peculiarities get smeared out.

16.3.3 Rocket Engines

We have shown that, in order to push a quasi-one-dimensional flow from subsonic to supersonic, one must send it through a throat. This result is exploited in the design of rocket engines and jet engines.

In a rocket engine, hot gas is produced by controlled burning of fuel in a large chamber and escapes through a *converging-diverging* (also known as *De Laval*) nozzle, as shown in Fig. 16.5. The nozzle is designed with a skirt so the flow becomes supersonic smoothly when it passes through the nozzle's throat.

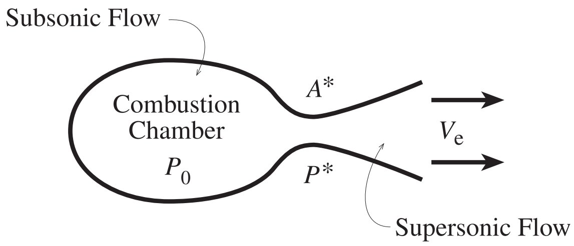

Fig. 16.5: Schematic illustration of a rocket engine. Note the skirt, which increases the thrust produced by the escaping exhaust gases.

To analyze this flow in some detail, let us approximate it as precisely steady and isentropic, and the gas as perfect (no viscosity) with constant ratio of specific heats γ. In this case, the enthalpy is $h = c^2/(\gamma - 1)$ [Eq. (16.8)], so Bernoulli's theorem (16.11) reduces to

$$\frac{c^2}{(\gamma-1)} + \frac{1}{2}v^2 = \frac{c_0^2}{(\gamma-1)} . \tag{16.15}$$

Here c is the sound speed in the flow and c_0 is the "stagnation" sound speed, i.e., the sound speed evaluated in the rocket chamber where $v = 0$. Dividing this Bernoulli theorem by c^2 and manipulating, we learn how the sound speed varies with Mach number $M = v/c$:

$$c = c_0 \left[1 + \frac{\gamma-1}{2}M^2\right]^{-1/2} . \tag{16.16}$$

From mass conservation [Eq. (16.9)], we know that the cross sectional area A varies as $A \propto \rho^{-1}v^{-1} \propto \rho^{-1}M^{-1}c^{-1} \propto M^{-1}c^{(\gamma+1)/(1-\gamma)}$, where we have used $\rho \propto c^{2/(\gamma-1)}$ [Eq. (16.8)]. Combining with Eq. (16.16), and noting that $M = 1$ where $A = A_*$ (i.e., the flow is transonic at the throat), we find that

$$\frac{A}{A_*} = \frac{1}{M}\left[\frac{2}{\gamma+1} + \left(\frac{\gamma-1}{\gamma+1}\right)M^2\right]^{\frac{(\gamma+1)}{2(\gamma-1)}} , \tag{16.17}$$

The pressure P_* at the throat can be deduced from $P \propto \rho^\gamma \propto c^{2\gamma/(\gamma-1)}$ [Eqs. (16.5) and (16.8)] together with Eq. (16.16) with $M = 0$ and $P = P_0 =$ (stagnation pressure) in the chamber and $M = 1$ at the throat:

$$P_* = P_0 \left(\frac{2}{\gamma+1}\right)^{\frac{\gamma}{\gamma-1}} . \tag{16.18}$$

We use these formulas in Box 16.1 and Ex. 16.2 to evaluate, numerically, some features of the space shuttle and its rocket engines.

Bernoulli's theorem is a statement that energy is conserved along a streamtube. However, momentum is not conserved. As a subsonic flow accelerates and the area of the streamtube diminishes, the momentum flowing per second along the streamtube, $(P + \rho v^2)A$, decreases. This is due to the pressure force acting normally on the converging surface of the streamtube and removing momentum from the flow. As a result, if the rocket did not have a skirt, but instead opened up completely to the outside world at the throat, the resulting rocket thrust,

$$T_* = (P_* + \rho_* v_*^2)A_* = 8P_*A_*/3 \ , \tag{16.19}$$

would be less than if momentum were conserved along the subsonic, accelerating streamtubes.

Much of the "lost" momentum can be regained, and the thrust can thus be made significantly larger than T_*, by adding a "skirt" behind the throat as shown in Fig. 16.5. The nozzle's skirt keeps the flow quasi-one-dimensional well beyond the throat, driving it more and more strongly supersonic. In this accelerating, supersonic flow each tube's momentum flow $(P + \rho v^2)A$ increases downstream, and there is a compensating increase of the rocket's forward thrust. This skirt-induced force accounts for a significant fraction of the thrust of a well-designed rocket engine.

Rockets work most efficiently when the exit pressure of the gas, as it leaves the base of the skirt, matches the external pressure in the surrounding air. When the pressure in the exhaust is larger than the external pressure, the flow is termed $under - expanded$ and a pulse of low pressure, known as a *rarefaction* will be driven into the escaping gases causing them to expand and increasing their speed. However, the exhaust will now be pushing on the surrounding air, rather than on the rocket. More thrust could have been exerted on the rocket if the flow had not been under-expanded. By contrast, when the exhaust has a smaller pressure that the surrounding air (i.e., is *over-expanded*), shock fronts will form near the exit of the nozzle, affecting the fluid flow and sometimes causing separation of the flow from the nozzle's walls. It is important that the nozzle's skirt be shaped so that the exit flow is neither seriously over- or under-expanded.

****

EXERCISES

Exercise 16.1 *Derivation: de Laval Nozzle*
Verify Eqs. (16.13) and (16.18).

Exercise 16.2 *Problem: Space Shuttle s Solid-Fuel Boosters*
Use the rough figures in Box 16.1 to estimate the energy released per unit mass in burning the fuel. Does your answer seem reasonable to you?

****

16.4 One Dimensional, Time-Dependent Flow

16.4.1 Riemann Invariants

Let us turn now to time-dependent flows. Again we confine our attention to the simplest situation that illustrates the physics, in this case, truly one-dimensional motion of an isentropic

Box 16.1
Space Shuttle

The Space Shuttle provides many convenient examples of the behavior of supersonic flows. At launch, the shuttle and fuel have a mass $\sim 2 \times 10^6$ kg. The maximum thrust, $T \sim 3 \times 10^7$N, occurs at lift-off and lifts the rocket with an initial acceleration relative to the ground of $\sim 0.5g_e$. This increases to $\sim 3g_e$ as the fuel is burned and the total mass diminishes. Most of the thrust is produced by two solid-fuel boosters which burn fuel at a combined rate of $\dot{m} \sim 10000$ kg s^{-1} over a two minute period. They produce a combined thrust of $T \sim 2 \times 10^7$N averaged over the two minutes, from which we can estimate the speed of the escaping gases as they leave the exhaust. Assuming that this speed is quite supersonic, we estimate that $V_e \sim T/\dot{m} \sim 2$km s^{-1} . Now the combined exit areas of the two exhausts is $A_e \sim 20$m^2, roughly four times the throat area, A_*. Using Eq. (16.13), we deduce that the exit Mach number is $M_e \sim 3$.

The exit pressure is $P_e \sim T/\gamma M_e^2 \sim 8 \times 10^4$ N m^{-2}, about atmospheric. The stagnation pressure within the combustion region is roughly

$$P_0 \sim \left[1 + \frac{(\gamma-1)M_e^2}{2}\right]^{\frac{\gamma}{\gamma-1}} \sim 35 \text{ atmospheres.} \quad (1)$$

Of course the actual operation is far more complex than this. For example, to optimize the final altitude, one must allow for the decreasing mass and atmospheric pressure as well as the two dimensional gas flow through the nozzle.

The space shuttle can also be used to illustrate the properties of shock waves (Sec. 16.5). When the shuttle re-enters the atmosphere it is traveling highly supersonically. It must therefore be preceded by a strong shock front which heats the onrushing air and consequently heats the shuttle. The shuttle continues moving supersonically until it reaches an altitude of 15km and until this time creates a shock wave pattern that can be heard on the gound as a sonic boom. The maximum heating rate occurs at an altitude of 70km. Here, the shuttle moves at $V \sim 7$km s^{-1} and the sound speed is about 280 m s^{-1}, giving a Mach number of 25. If we adopt a specific heat ratio $\gamma \sim 1.5$ and a mean molecular weight $\mu \sim 10$ appropriate to dissociated air, we can conclude from the Rankine-Hugoniot conditions and the ideal gas law, Eq. (4) of Box 12.1, that the post shock temperature is

$$T \sim \frac{2(\gamma-1)\mu m_p V^2}{(\gamma+1)^2 k} \sim 9000\text{K} \quad (2)$$

Exposure to gas at this high a temperature heats the nose to $\sim 1800K$.

There is a second, well-known consequence of this high temperature and that is that it is sufficient to ionise the air partially as well as dissociate it. This surrounds the shuttle with a sheath of plasma, which as we shall discover in chapter 18, prevents radio communication. The blackout is maintained for about 12 minutes.

fluid in the absence of viscosity, thermal conductivity and gravity. The motion of the gas in such a flow is described by the equation of continuity and the Euler equation specialized to one dimension.

$$\frac{d\rho}{dt} = -\rho\frac{\partial v}{\partial x}\ ,$$
$$\frac{dv}{dt} = -\frac{1}{\rho}\frac{\partial P}{\partial x}\ , \tag{16.20}$$

where

$$\frac{d}{dt} = \frac{\partial}{\partial t} + v\frac{\partial}{\partial x} \tag{16.21}$$

is the convective derivative.

Given an isentropic equation of state $P = P(\rho)$ to relate the pressure to the density, these two non-linear equations can be combined into a single second order differential equation in the velocity. However, it is more illuminating to work with the first-order set. As the gas is isentropic, the density ρ and sound speed $c = (dP/d\rho)^{1/2}$ can both be regarded as functions of a single thermodynamic variable which we choose to be the pressure.

Taking linear combinations of Eqs. (16.20), we obtain two equivalent partial differential equations

$$\frac{\partial v}{\partial t} \pm \frac{1}{\rho c}\frac{\partial P}{\partial t} + (v \pm c)\left(\frac{\partial v}{\partial x} \pm \frac{1}{\rho c}\frac{\partial P}{\partial x}\right) = 0\ . \tag{16.22}$$

It is enlightening to rewrite these equations in terms of *Riemann invariants*

$$J_\pm \equiv v \pm \int \frac{dP}{\rho c} \tag{16.23}$$

and the *characteristic speeds*

$$V_\pm \equiv v \pm c. \tag{16.24}$$

The result is

$$\left(\frac{\partial}{\partial t} + V_\pm\frac{\partial}{\partial x}\right) J_\pm = 0. \tag{16.25}$$

Equation (16.25) tells us that the convective derivative of each Riemann invariant $J_\pm$ vanishes for an observer who moves, not with the fluid speed, but, instead, with the speed $V_\pm$. We say that each Riemann invariant is conserved along its characteristic (denoted by $C_\pm$) which is a path through spacetime satisfying

$$C_\pm : \quad \frac{dx}{dt} = v \pm c. \tag{16.26}$$

Note that in these equations, both v and c are functions of x and t.

The characteristics have a natural interpretation. They describe the motion of small disturbances traveling backward and forward relative to the fluid at the local sound speed. As seen in the fluid's local rest frame $v = 0$, two neighboring events in the flow, separated by a small time interval Δt and a space interval $\Delta x = +c\Delta t$ so that they lie on the same C_+ characteristic, will have small velocity and pressure differences satisfying $\Delta v = -\Delta P/\rho c$

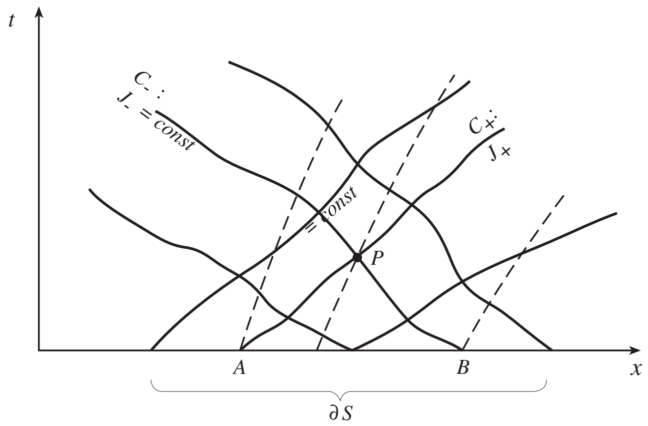

Fig. 16.6: Spacetime diagram showing the characteristics (solid lines) for a one dimensional flow of an isentropic gas. The paths of the fluid elements are shown as dashed lines. Initial data are presumed to be specified over some interval ∂S of x at time $t = 0$. The Riemann invariants J_+ is constant along the characteristic C_+ and thus at point P it has the same value, unchanged, as at point A in the initial data. Similarly J_- at P has the same value as at B. The shaded area of spacetime is the domain of dependence S of ∂S

[as one can deduce from Eqs. (16.20) with $v = 0$, $d/dt = \partial/\partial t$ and $c^2 = dP/d\rho$]. Now, for a linear sound wave, propagating along the positive x direction, Δv and ΔP will separately vanish. However in a nonlinear wave, only the combination $\Delta J_+ = \Delta v + \Delta P/\rho c$ will vanish along C_+. Integrating over a finite interval of time, we recover the constancy of J_+ along the characteristic C_+ [Eq. (16.23)].

The Riemann invariants provide a general method for solving the initial value problem. Suppose that the fluid velocity and the thermodynamic variables are specified over an interval of x, designated ∂S at an initial time $t = 0$ [Fig. 16.6]. This means that $J_\pm$ are also specified over this interval. We can then determine $J_\pm$ at any point P in the *domain of dependence* S of ∂S (i.e., at any point linked to ∂S by two characteristics $C_\pm$) by simply propagating each of $J_\pm$ unchanged along its characteristic. From these values of $J_\pm$ at P, we can solve algebraically for all the other flow variables (v, P, ρ, ...) at P. To learn the evolution outside the domain of dependence S, we must specify the initial conditions outside ∂S.

We can use Riemann invariants to understand qualitatively how a nonlinear sound wave evolves with time. If the wave propagates in the positive x direction into previously undisturbed fluid (fluid with $v = 0$), then the J_- invariant, propagating backward along C_-, is constant everywhere, so $v = \int dP/\rho c +$ constant. Let us use $q \equiv \int dP/\rho c$ as our wave variable. For a perfect gas with constant ratio of specific heats γ, $q = 2c/(\gamma - 1)$, so our oscillating wave variable is essentially the oscillating sound speed. Constancy of J_- then says that $v = q - q_0$, where q_0 is the stagnation value of q, i.e. the value of q in the undisturbed fluid.

Now, $J_+ = v + q$ is conserved on each rightward characteristic C_+, and so both v and q are separately conserved on each C_+. If we sketch a profile of the wave pulse as in Fig. 16.7 and measure its amplitude using the quantity q, then the relation $v = q - q_0$ says that the fluid at the crest of the wave moves faster than the fluid in a trough. This causes the leading edge

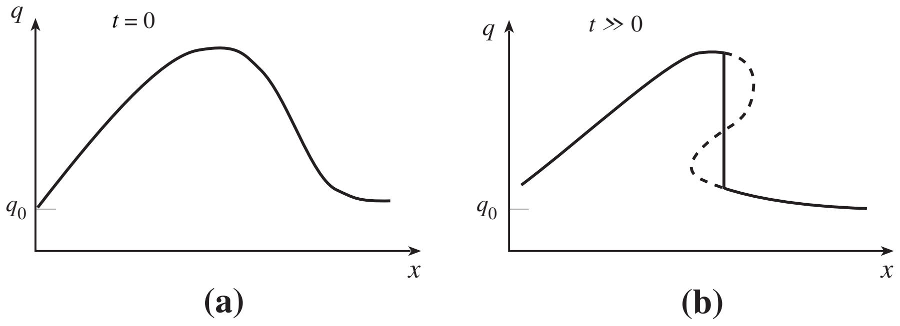

Fig. 16.7: Evolution of a nonlinear sound wave. The fluid at the crest of the wave moves faster than the fluid in the trough. Mathematically, the flow eventually becomes triple-valued. Physically, a shock wave develops.

of the wave to steepen, a process we have already encountered in our discussion of shallow-water solitons (Chap. 15). Now, sound waves, by constrast with shallow-water waves, are non-dispersive so the steepening will continue until $|dv/dx| \to \infty$ (Fig. 16.7). When the velocity gradient becomes sufficiently large, viscosity and dissipation will become strong, producing an increase of entropy and a breakdown of our isentropic flow. This breakdown and entropy increase will occur in an extremely thin region—a shock wave, which we shall study in Sec. 16.5

16.4.2 Shock Tube

We have shown how one dimensional isentropic flows can be completely analyzed by propagating the Riemann invariants along characteristics. Let us illustrate this in more detail by analyzing a shock tube, a laboratory device for creating supersonic flows and studying the behavior of shock waves. In a shock tube, high pressure gas is retained at rest in the left half of a long tube by a thin membrane. At time $t = 0$, the membrane is ruptured by a laser beam and the gas rushes into the tube's right half, which has usually been evacuated. Diagnostic photographs and velocity and pressure measurements are synchronised with the onset of the flow.

Let us idealize the operation of a shock tube by assuming, once more, that the gas is perfect with constant γ, so that $P \propto \rho^\gamma$. For times $t \le 0$, we suppose that the gas has uniform density ρ_0 and pressure P_0 (and consequently uniform sound speed c_0) at $x \le 0$, and that $\rho = P = 0$ at $x \ge 0$. At time $t = 0$, the barrier is removed and the gas flows towards positive x. Now, the first Riemann invariant J_+ is conserved on C_+, which originates in the static gas, so it has the value

$$J_+ = v + \frac{2c}{\gamma - 1} = \frac{2c_0}{\gamma - 1}\ . \tag{16.27}$$

Note that in this case, the invariant is the same on all rightward characteristics, i.e. throughout the flow, so

$$v = \frac{2(c - c_0)}{\gamma - 1} \quad \text{everywhere.} \tag{16.28}$$

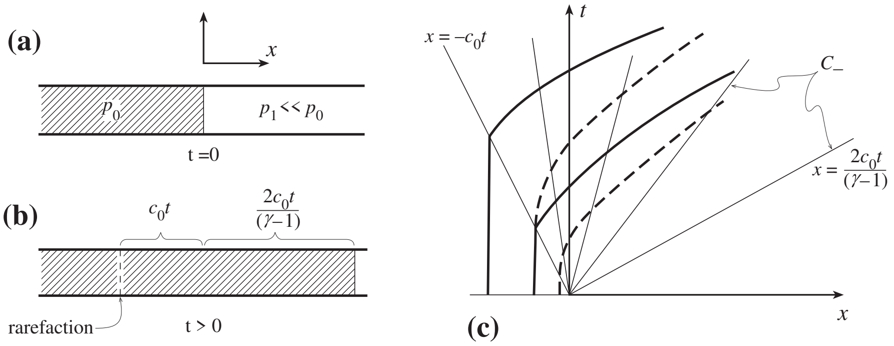

Fig. 16.8: Shock Tube. (a) At $t \leq 0$ gas is held at rest at high pressure P_0 in the left half of the tube. (b) At $t > 0$ the high-pressure gas moves rightward down the tube at high speed, and a rarefaction wave propagates leftward at the sound speed. (c) This graph shows the flow's characteristics (C_+: thin dashed lines; C_-: thin solid lines) and fluid paths (thick solid lines).

The second invariant is

$$J_- = v - \frac{2c}{\gamma - 1} \, . \tag{16.29}$$

Its constant values are not so easy to identify because those characteristics C_- that travel through the perturbed flow all emerge from the origin, where v and c are indeterminate; cf. Fig. 16.8. However, by combining Eq. (16.28) with Eq. (16.29), we deduce that v and c are separately constant on each characteristic C_-. This enables us, trivially, to solve the differential equation $dx/dt = v - c$ for the leftward characteristics C_-, obtaining

$$C_- : \quad x = (v - c)t \, . \tag{16.30}$$

Here we have set the constant of integration equal to zero so as to obtain all the characteristics that propagate through the perturbed fluid. (For those in the unperturbed fluid, $v = 0$ and $c = c_0$, so $x = x_0 - c_0 t$ with $x_0 < 0$ the characteristic's initial location.)

Now Eq. (16.30) is true on each characteristic in the perturbed fluid. Therefore it is true throughout the perturbed fluid. We can therefore combine Eqs. (16.29), (16.30) to solve for $v(x,t)$ and $c(x,t)$ throughout the perturbed fluid. That solution, together with the obvious solution (same as initial data) to the left and right of the perturbed fluid, is:

$$\begin{aligned}
&v = 0 \, , \quad c = c_0 \quad \text{at } x < -c_0 t \, , \\
&v = \frac{2}{\gamma+1}\left(c_0 + \frac{x}{t}\right) \, , \quad c = \frac{2c_0}{\gamma+1} - \left(\frac{\gamma-1}{\gamma+1}\right)\frac{x}{t} \quad \text{at } -c_0 t < x < \frac{2c_0}{\gamma-1}t \, , \\
&\text{vacuum prevails at } x > \frac{2c_0}{\gamma-1}t \, .
\end{aligned} \tag{16.31}$$

Notice, in this solution, that the gas at $x < 0$ remains at rest until a *rarefaction wave* from the origin reaches it. Thereafter it is accelerated rightward by the local pressure gradient, and as it accelerates it expands and cools so its speed of sound c goes down; asymptotically it reaches zero temperature as exhibited by $c = 0$ and an asymptotic speed $v = 2c_0/(\gamma - 1)$ [cf. Eq. (16.27)]; see Fig. 16.8. In the expansion, the internal random velocity of the gas molecules is transformed into an ordered velocity just as in a rocket's exhaust. However, the total energy per unit mass in the stationary gas is $u = c_0^2/\gamma(\gamma-1)$ [Eq. (16.8)], which is less than the asymptotic kinetic energy per unit mass of $2c_0^2/(\gamma-1)^2$. The missing energy has gone into performing work on the gas that is still struggling to reach its asymptotic speed.

In the more realistic case where there initially is some low-density gas in the evaculated half of the tube, the expanding driver gas creates a strong shock as it plows into the low-density gas. In the next section we shall explore the structure of this and other shock fronts.

****

EXERCISES

Exercise 16.3 *Problem: Fluid Paths in Free Expansion*
We have computed the velocity field for a freely expanding gas, Eq. (16.31). Use this result to show that the path of an individual fluid element is

$$x = \frac{2c_0 t}{\gamma-1} + \left(\frac{\gamma+1}{\gamma-1}\right) x_0 \left(\frac{-c_0 t}{x_0}\right)^{\frac{2}{\gamma+1}} \quad \text{at } 0 < -x_0/c_0 < t \, .$$

****

16.5 Shock Fronts

We have just demonstrated that in an ideal fluid, large perturbations to fluid dynamical variables inevitably evolve to form a divergently large velocity gradient—a *shock front*. Now, when the gradient becomes large, we can no longer ignore the viscous stress because the viscous terms in the Navier-Stokes equation involve second derivatives in space, whereas the inertial term involves only first derivatives. As in turbulence and in boundary layers, so also in a shock front, the viscous stress converts the fluid's ordered, bulk kinetic energy into microscopic kinetic energy, i.e. thermal energy. The ordered fluid velocity $\mathbf{v}$ thereby is rapidly—almost discontinuously—reduced from supersonic to subsonic, and the fluid is heated. The cooler, supersonic region of incoming fluid is said to be *ahead of* or *upstream from* the shock; the hotter, subsonic region of outgoing fluid is said to be *behind* or *downstream from* the shock.

The viscosity is crucial to the internal structure of the shock, but it is just as negligible in the downstream flow behind the shock as in the upstream flow ahead of the shock, since there velocity gradients are modest again. Remarkably, if (as is usually the case) the shock front is very thin compared to the length scales in the upstream and downstream flows, and the time for the fluid to pass through the shock is short compared to the upstream and downstream timescales, then we can deduce the net influence of the shock on the flow without any reference to the viscous processes that operate within the shock, and without reference to the shock's detailed internal structure. We do so by treating the shock as a discontinuity across which certain junction conditions must be satisfied. This is similar to electromagnetic theory, where the junction conditions for the electric and magnetic fields across a material interface are independent of the detailed structure of the interface.

The keys to the shock's junction conditions are the conservation laws for mass, momentum and energy: The fluxes of mass, momentum, and energy must usually be the same in the downstream flow, emerging from the shock, as in the upstream flow, entering the shock. To understand this, we first note that, because the time to pass through the shock is so short, the flow can be regarded as stationary. In a stationary flow the mass flux is always constant (at least in non-relativistic fluid dynamics), as there is no way to create new mass; its continuity across the shock can be written as

$$[\rho \mathbf{v} \cdot \mathbf{n}] = 0 \, , \tag{16.32}$$

where $\mathbf{n}$ is the unit normal to the shock front and the square bracket means the difference in the values on the downstream and upstream sides of the shock. Similarly, the total momentum flux, $\mathsf{T} \cdot \mathbf{n}$, must be conserved in the absence of external forces. Now T has both a mechanical component, $P\mathbf{g} + \rho \mathbf{v} \otimes \mathbf{v}$ and a viscous component, $-\zeta\theta\mathbf{g} - 2\eta\boldsymbol{\sigma}$. However, the viscous component is negligible in the upstream and downstream flows, which are being matched to each other, so the mechanical component by itself must be conserved across the shock front:

$$[(P\mathbf{g} + \rho \mathbf{v} \otimes \mathbf{v}) \cdot \mathbf{n}] = 0 \, . \tag{16.33}$$

Similar remarks apply to the energy flux, though here we must be slightly more restrictive. There are three ways that a change in the energy flux could occur. First, energy may be added to the flow by chemical or nuclear reactions that occur in the shock front. Second, the gas may be heated to such a high temperature that it will lose energy through the emission of radiation. Third, energy may be conducted far upstream by suprathermal particles so as to pre-heat the incoming gas. This will thicken the shock front and may make it so thick that it can no longer be sensibly approximated as a discontinuity. If any of these processes are occuring, we must check to see whether they are strong enough to significantly influence energy conservation across the shock. What such a check often reveals is that preheating is negligible, and the lengthscales over which the chemical and nuclear reactions and radiation emission operate are much greater than the length over which viscosity acts. In this case we can conserve energy flux across the viscous shock and then follow the evolutionary effects of reactions and radiation (if significant) in the downstream flow.

A shock with negligible preheating, and with neglible radiation emission and chemical and nuclear reactions inside the shock, will have the same energy flux in the departing, downstream flow as in the entering, upstream flow, i.e., they will satisfy

$$\left[\left(\frac{1}{2}v^2 + h\right) \rho \mathbf{v} \cdot \mathbf{n}\right] = 0 \, . \tag{16.34}$$

Shocks which satisfy the conservation laws of mass, momentum and energy, Eqs. (16.32), (16.33) and (16.34), are said to be *adiabatic*.

By contrast, with mass, momentum and energy, the flux of entropy will not be conserved across a shock front, since viscosity and other dissipative processes increase the entropy as the fluid flows through the shock. So far, the only type of dissipation which we have discussed is viscosity and this is sufficient by itself to produce a shock front and keep it thin. However, heat conduction, which we shall analyze in the following chapter, and electrical resisitivity, which is important in magnetic shocks (Chap. 18), can also contribute to the dissipation and can influence the detailed structure of the shock front.

For an adiabatic shock, the three requirements of mass, momentum and energy conservation, known collectively as the *Rankine-Hugoniot relations*, enable us to relate the downstream flow and its thermodynamic variables to their upstream counterparts.[1]

Let us work in the reference frame in which the shock front is at rest and in which the flow is stationary, and let us simplify matters by assuming that the upstream flow is normally incident upon the shock front. (A Galilean transformation along the shock front can accomplish this.) We use the subscripts 1, 2 to denote quantities measured ahead of and behind the shock respectively; i.e., 1 is the incoming flow and 2 is the outgoing flow. The Rankine-Hugoniot relations (16.32), (16.33) and (16.34) then take the forms

$$\begin{aligned} \rho_2 v_2 &= \rho_1 v_1 = j \ , \\ P_2 + \rho_2 v_2^2 &= P_1 + \rho_1 v_1^2 \ , \\ h_2 + \frac{1}{2} v_2^2 &= h_1 + \frac{1}{2} v_1^2 \ , \end{aligned} \tag{16.35}$$

where j is the mass flux, which is determined by the upstream flow.

These equations can be brought into a more useful form by replacing the density with the *specific volume* $V \equiv 1/\rho$, replacing the enthalpy by its value in terms of P and V, $h = u + P/\rho = u + PV$ [Eq. (16.35)], and performing some algebra; the result is

$$\begin{aligned} j^2 &= \frac{P_2 - P_1}{V_1 - V_2} \ , \\ v_1 - v_2 &= [(P_2 - P_1)(V_1 - V_2)]^{1/2} \ , \\ u_2 - u_1 &= \frac{1}{2}(P_1 + P_2)(V_1 - V_2) \ . \end{aligned} \tag{16.36}$$

This is the most widely used form of the Rankine-Hugoniot relations. It must be augmented by the equation of state in the form

$$u = u(P, V) \ . \tag{16.37}$$

Some of the physical content of these Rankine-Hugoniot relations is depicted in Fig. 16.9. The thermodynamic state of the upstream (incoming) fluid is the point (V_1, P_1) in this volume-pressure diagram. The thick solid curve, called the *shock adiabat*, is the set of all possible downstream (outgoing) fluid states. This shock adiabat can be computed by combining the third of Eqs. (16.36) with the equation of state (16.37). Those equations will actually give a curve that extends away from (V_1, P_1) in both directions, up-leftward

[1] The existence of shocks was actually understood quite early on, more or less in this way, by Stokes. However, he was persuaded by his former student Rayleigh that such discontinuities were impossible because they would violate energy conservation. With a deference that professors traditionally show their students, Stokes believed him.

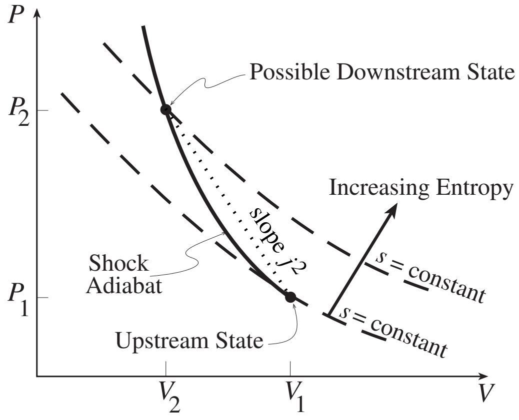

Fig. 16.9: Shock Adiabat. The pressure specific volume $V = 1/\rho$ in the upstream flow are P_1 and V_1, and in the downstream flow P_2 and V_2. The dashed curves are ordinary adiabats (curves of constant entropy per unit mass s). The thick curve is the *shock adiabat*, the curve of allowed upstream states (V_1, P_1) for a given downstream state (V_2, P_2). The actual location of the downstream state on this adiabat is determined by the mass flux j flowing through the shock: the slope of the dotted line connecting the upstream and downstream states is j^2.

and down-rightward. Only the up-leftward portion is compatible with an increase of entropy across the shock; the down-righward portion requires an entropy decrease, which is forbidden by the second law of thermodynamics, and therefore is not drawn on the diagram. The actual location (V_2, P_2) of the downstream state along the shock adiabat is determined by the first of the Rankine-Hugoniot relations (16.36) in a simple way: the slope of the dotted line connecting the upstream and downstream states is $-j^2$, where j is the mass flux passing through the shock. When one thereby has learned (V_2, P_2), one can compute the downstream speed v_2 from the second of the Rankine-Hugoniot relations (16.36).

It can be shown that the pressure and density always increase across a shock (as is the case in Fig. 16.9), and the fluid always decelerates,

$$P_2 > P_1 \ , \quad V_2 < V_1 \ , \quad v_2 < v_1 \ ; \tag{16.38}$$

see Ex. 16.7. It can also be demonstrated in general, and will be verified in a particular case below, that the Rankine-Hugoniot relations require the flow to be supersonic with respect to the shock front upstream $v_1 > c_1$ and subsonic downstream, $v_2 < c_2$. Physically, this is sensible (as we have seen above): When the fluid approaches the shock supersonically, it is not possible to communicate a pressure pulse upstream (via a Riemann invarient moving at the speed of sound) and thereby cause the flow to decelerate, and so a shock must develop.[2] Similarly, the shock front can only respond to changes in the downstream conditions, as it must, if it is in causal contact with the downstream flow, and causal contact requires that the flow be subsonic so a Riemann invariant can propagate upstream to the shock.

Although they are often regarded as discontinuities, shocks, like boundary layers, do have structure. The simplest case is that of a gas in which the shear viscosity coefficient

[2]Of course, if there is some faster means of communication, for example photons or, in an astrophysical context, cosmic rays, then there may be a causal contact between the shock and the inflowing gas, and this can either prevent shock formation or lead to a more complex shock structure.

is molecular in origin and is given by $\eta = \rho\nu \sim \rho l_{\rm mfp}\bar{v}_{\rm th}/3$, where $l_{\rm mfp}$ is the mean free path and $v_{\rm th} \sim c$ is the thermal speed of the molecules. In this case the viscous stress $T_{xx} = -\zeta\theta - 2\eta\sigma_{xx}$ is $-(\zeta + 4\eta/3)dv/dx$, where ζ is the coefficient of bulk viscosity which can be of the same order as the coeffient of shear viscosity. In the shock, this must roughly balance the total kinetic momentum flux $\sim \rho v^2$. If we estimate the velocity gradient dv/dx by v_1/δ_S where δ_S is a measure of the shock thickness and we estimate the sound speed in the shock front by $c \sim v_1$, then we deduce that the shock thickness is $\delta_S \sim l_{\rm mfp}$, the collision mean free path in the gas. For air at standard temperature and pressure, the mean free path is $l_{\rm mfp} \sim (\sqrt{2}n\pi\sigma^2)^{-1} \sim 70$ nm, where n is the molecular density and σ is the molecular diameter. This is very small! Microscopically, it makes sense that $\delta_S \sim l_{\rm mfp}$ as an individual molecule only needs a few collisions to have its ordered motion perpendicular to the shock front randomized. However, this estimate raises a problem as it brings into question our use of the continuum approximation (cf. Sec. 12.1). It turns out that, when a more careful calculation of the shock structure is carried out incorporating heat conduction, the shock thickness is several mean free paths, fluid dynamics is acceptable for an approximate theory, and the results are in rough accord with measurements of the velocity profiles of shocks with modest Mach numbers. Despite this, a kinetic treatment is usually necessary for an accurate description of the shock structure.

So far we have assumed that the shocked fluid is made of uncharge molecules. A more complicated type of shock can arise in an ionized gas, i.e. a plasma (Part V). Shocks in the solar wind are examples. In this case, the collision mean free paths are enormous, in fact comparable with the transverse size of the shock, and therefore one might expect the shocks to be so thick that the Rankine-Hugoniot relations will fail. However, spacecraft measurements reveal solar-wind shocks that are relatively thin—far thinner than than the collisional mean free paths of the plasma's electrons and ions. In this case, it turns out that collisionless, collective interactions in the plasma are responsible for the viscosity and dissipation. These processes are so efficient that thin shock fronts can occur without individual particles having to hit one another. Since the shocks are thin, they must satisfy the Rankine-Hugoniot relations. We shall discuss collisionless shocks further in Chap. 20.

To summarize, shocks are machines that decelerate a normally incident upstream flow to a subsonic speed, so it can be in causal contact with conditions downstream. In the process, bulk momentum flux, ρv^2, is converted into pressure, bulk kinetic energy is converted into internal energy, and entropy is manufactured by the dissipative processes at work in the shock front. For a given shock Mach number, the downstream conditions are fixed by the conservation laws of mass, momentum and energy and are independent of the detailed dissipation mechanism.

16.5.1 Shock jump conditions in a perfect gas

Let us again specialize to a perfect gas with constant specific-heat ratio γ, so the equation of state is $u = PV/(\gamma - 1)$ and the sound speed is $c = \sqrt{\gamma P/\rho} = \sqrt{\gamma PV}$ [Eqs. (16.5)–(16.8)]. We measure the strength of the shock using the *shock Mach number* M, which is defined to be the Mach number in the upstream flow, $M \equiv M_1 = v_1/c_1 = \sqrt{v_1^2/\gamma P_1 V_1}$. With the aid of this equation of state and Mach number, we can bring the Rankine-Hugoniot relations

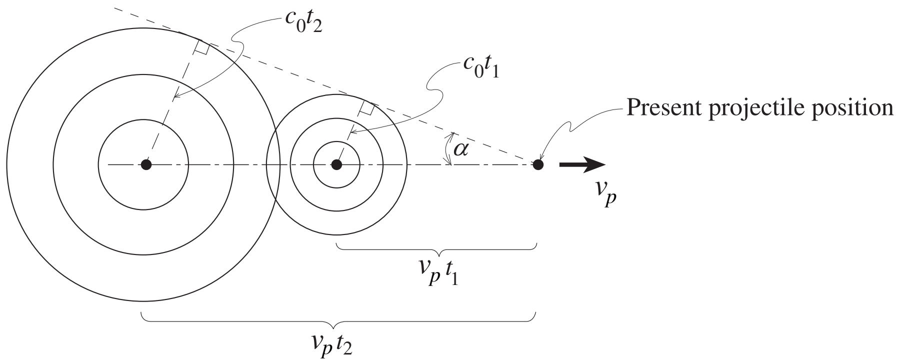

Fig. 16.10: Construction for Mach cone formed by a supersonic projectile. The cone angle is $\alpha = \sin^{-1}(M^{-1})$, where $M - v_p/c_0$ is the Mach number of the projectile.

(16.36) into the form

$$\frac{V_2}{V_1} = \frac{v_2}{v_1} = \frac{\gamma-1}{\gamma+1} + \frac{2}{(\gamma+1)M^2} , \tag{16.39}$$

$$\frac{P_2}{P_1} = \frac{2\gamma M^2}{\gamma+1} - \frac{\gamma-1}{\gamma+1} , \tag{16.40}$$

and

$$M_2^2 = \frac{2+(\gamma-1)M^2}{2\gamma M^2 - (\gamma-1)} . \tag{16.41}$$

Here $M_2 \equiv v_2/c_2$ is the downstream Mach number.

The results for this equation of state illustrate a number of general features of shocks: The density and pressure increase across the shock, the speed decreases, and the downstream flow is subsonic—all discussed above—and one important new feature: A shock weakens as its Mach number M decreases. In the limit that $M \to 1$, the jumps in pressure, density, and speed vanish and the shock disappears.

In the strong-shock limit, $M \gg 1$, the jumps are

$$\frac{V_2}{V_1} = \frac{v_2}{v_1} \simeq \frac{\gamma-1}{\gamma+1} , \tag{16.42}$$

$$\frac{P_2}{P_1} \simeq \frac{2\gamma M^2}{\gamma+1} . \tag{16.43}$$

Thus, the density jump is always of order unity, but the pressure jump grows ever larger as M increases. Air has $\gamma \simeq 1.4$, so the density compression ratio for a strong shock in air is 6 and the pressure ratio is $P_2/P_1 = 1.2M^2$

16.5.2 Mach Cone

The shock waves formed by a supersonically moving body are quite complex close to the body and depend on its detailed shape, Reynolds' number, etc. However, far from the body, the leading shock has the form of the *Mach cone* shown in Fig. 16.10. We can understand

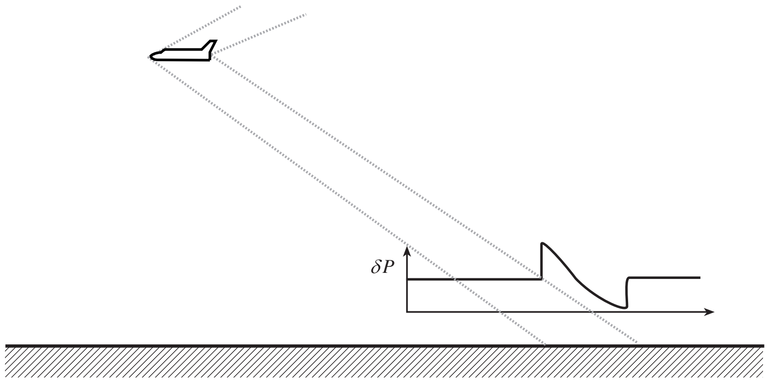

Fig. 16.11: Double shock created by supersonic projectile and associated "N wave" pressure distribution.

this cone by the construction shown in the figure. The shock is the boundary between that fluid which is in sound-based causal contact with the projectile and that which is not. This boundary is mapped out by (conceptual) sound waves that propagate into the fluid from the projectile at the ambient sound speed c_0. When the projectile is at the indicated position, the envelope of these circles is the shock front and has the shape of the Mach cone, with opening angle (the *Mach angle*)

$$\alpha = \sin^{-1}(\frac{1}{M}) . \tag{16.44}$$

Usually, there will be two such shock cones, one attached to the projectile's bow shock and the other formed out of the complex shock structure in its tail region. The pressure must jump twice, once across each of these shocks, and will therefore form an *N wave* which propagates cylindrically away from the projectile as shown in Fig. 16.11. Behind the first shock, the density and pressure drop off gradually by more than the first shock's compression. As a result, the fluid flowing into the second shock has a lower pressure, density, and sound speed than that flowing into the first (cf. Fig. 16.11). This causes the Mach number of the second shock to be higher than that of the first, and its Mach angle thus to be smaller. As a result, the separation between the shocks increases as they travel—$\propto r^{1/4}$ it turns out, where r is the perpendicular distance of the point of observation from the projectile's trajectory. In order to conserve energy flux the wave amplitude will then decrease $\propto r^{-3/4}$, rather than $\propto r^{-1/2}$ as would be true of a cylindrical sound pulse. Often a double boom can be heard on the ground.

****

EXERCISES

Exercise 16.4 *Problem: Speed of a Breaking Ocean Wave*
Consider an ocean wave approaching a gradually sloping beach and breaking as it progresses (Fig. 16.12). Assume that the water ahead of the breaking wave is at rest with respect to the beach and that the flow speed is independent of depth.

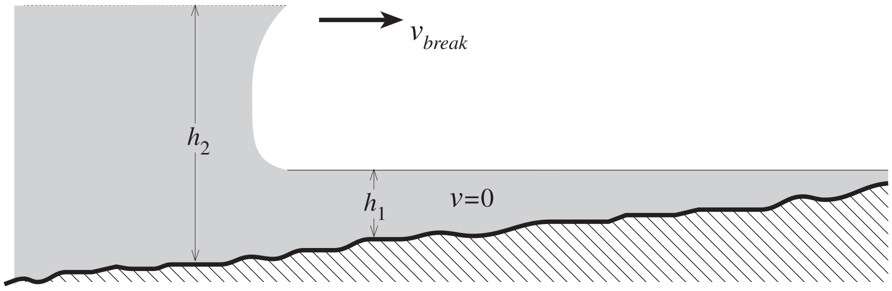

Fig. 16.12: Ocean wave breaking on a slowly sloping beach. The depth of water ahead of the wave is h_1 and the depth behind the wave is h_2.

(i) Compute the pressure as a function of depth ahead of and behind the wave. Conserve the total mass and momentum fluxes across the breaking wave to show that the wave moves with speed

$$v_{break} = \left[\frac{g(h_1 + h_2)h_2}{2h_1}\right]^{1/2}$$

relative to the water ahead of the wave. Hence calculate the mean speed of the water immediately following the wave.

(ii) We did not need to use energy conservation to obtain this result. Can you explain why?

(iii) Consider small-amplitude gravity waves in, the long wavelength limit, propagating ahead of and behind the breaking wave. Can the waves nearer the shore avoid being overtaken? Can those further from the shore catch up with the wave?

Exercise 16.5 *Problem: Shock Tube*
Consider a shock tube as discussed in Sec. 16.4 and Fig. 16.9. Suppose that there is a small density of gas at rest in the evacuated half of the tube, with specific heat ratio γ_1 which might differ from that of the driver gas, and with initial sound speed c_1. After the membrane is ruptured, the driver gas will expand into the evacuated half of the tube forming a shock front. Show that, in the limit of very large pressure ratio across the shock, the shock Mach number is

$$M_1 \simeq \left(\frac{\gamma_1 + 1}{\gamma - 1}\right)\left(\frac{c_0}{c_1}\right) ,$$

where c_0 is the driver gas's initial sound speed.

Exercise 16.6 *Problem: Sonic Boom from the Space Shuttle*
Use the quoted scaling of N wave amplitude with cylindrical radius r to make an order of magnitude estimate of the flux of acoustic energy produced by the space shuttle flying at Mach 2 at an altitude of 20km. Quote your answer in dB [cf. Eq. (15.76)].

Exercise 16.7 *Derivation and Challenge: Signs of Change Across a Shock*

(a) Almost all equations of state satisfy the condition $(\partial^2 V/\partial P^2)_s > 0$. Show that, when this is satisfied, the Rankine-Hugoniot relations and the law of entropy increase imply that the pressure and density must increase across a shock and the fluid must decelerate; i.e., $P_2 > P_1$, $V_2 < V_1$, and $v_2 < v_1$.

(b) Show that in a fluid that violates $(\partial^2 V/\partial P^2)_s > 0$, the pressure and density must still increase and the fluid decelerate across a shock, as otherwise the shock would be unstable.

For a solution to this exercise, see Sec. 84 of Landau and Lifshitz (1959).

****

16.6 Similarity Solutions — Sedov-Taylor Blast Wave

Strong explosions can generate shock waves. Examples include atmospheric nuclear explosions, supernova explosions, and depth charges. The debris a strong explosion will be at much higher pressure than the surrounding gas and will therefore drive a strong spherical shock into the surroundings. Initially, this shock wave will travel at roughly the radial speed of the expanding debris. However, the mass of fluid swept up by the shock will eventually exceed that of the explosion debris. The shock will then decelerate and the energy of the explosion will be transferred to the swept-up fluid. It is of obvious importance to be able to calculate how fast and how far the shock front will travel.

First make an order of magnitude estimate. Let the total energy of the explosion be E and the density of the surrounding fluid (assumed uniform) be ρ_0. Then after time t, when the shock radius is $R(t)$, the mass of swept-up fluid will be $\sim \rho_0 R^3$. The fluid velocity behind the shock will be roughly the radial velocity of the shock front, $v \sim \dot{R} \sim R/t$, and so the kinetic energy of the swept-up gas will be $\sim \rho_0 R^5/t^2$. There will also be internal energy in the post-shock flow, with energy density roughly equal to the post-shock pressure, $\rho u \sim P \sim \rho_0 \dot{R}^2$ [cf. the strong-shock jump condition (16.40) with $P_1 \sim \rho_0 c_0^2$ so $P_1 M^2 \sim \rho_0 v^2 \sim \rho_0 \dot{R}^2$]. The total internal energy within the expanding shock will then be $\sim \rho \dot{R}^2 R^3$, equal in order of magnitude to the kinetic energy. Equating either term to the total energy E of the explosion, we obtain the rough estimate

$$E = K \rho_0 R^5 t^{-2} , \tag{16.45}$$

which implies that at time t the shock front has reached the radius

$$R = \left(\frac{E}{K \rho_0} \right)^{1/5} t^{2/5} . \tag{16.46}$$

Here K is a numerical constant of order unity [not to be confused with the coefficient $K(s)$ in the equation of state (16.5)]. This scaling should hold roughly from the time that the mass of the debris is swept up to the time that the shock weakens to a Mach number of order unity so we can no longer use the strong-shock value $\sim \rho_0 \dot{R}^2$ for the post shock pressure.

Note that we could have obtained Eq. (16.46) by a purely dimensional argument as E and ρ_0 are the only significant controlling parameters in the problem. However, it is usually possible and always desirable to justify any such dimensional argument on the basis of the governing equations.

If, as we shall assume, the motion remains radial and the gas is perfect with constant specific-heat ratio γ, then we can solve for the details of the flow behind the shock front by integrating the radial flow equations

$$\begin{aligned} \frac{\partial \rho}{\partial t} + \frac{1}{r^2}\frac{\partial}{\partial r}(r^2 \rho v) &= 0 \, , \\ \frac{\partial v}{\partial t} + v\frac{\partial v}{\partial r} + \frac{1}{\rho}\frac{\partial P}{\partial r} &= 0 \, , \\ \frac{\partial}{\partial t}\left(\frac{P}{\rho^\gamma}\right) + v\frac{\partial}{\partial r}\left(\frac{P}{\rho^\gamma}\right) &= 0 \, . \end{aligned} \tag{16.47}$$

The first two equations are the familiar continuity equation and Euler equation written for a spherical flow. The third equation is energy conservation expressed as the adiabatic-expansion relation, $P \propto \rho^\gamma$ moving with a fluid element. Although P/ρ^γ is time-indendent for each fluid element, its value will change from element to element. Gas that has passed through the shock more recently will be given a smaller entropy than gas which was swept up when the shock was stronger, and thus will have a smaller value of P/ρ^γ.

Given suitable initial conditions, the partial differential equations (16.47) can be integrated numerically. However, there is a practical problem in that it is not easy to determine the initial conditions in an explosion! Fortunately, at late times, when most of the mass has been swept up, the fluid evolution is independent of the details of the initial expansion and in fact can be understood analytically as a *similarity solution*. By this, we mean that the shape of the radial profiles of pressure, density and velocity are independent of time.

We have already seen some examples of similarity solutions. The first was the Blasius solution for the structure of a laminar boundary layer (Sec. 13.4). In this case we argued on the basis of mass and momentum conservation that the thickness of the boundary layer as a function of distance x downstream would be $\sim \delta = (\nu x/V)^{1/2}$ where V was the speed of the flow above the boundary layer. This motivated us to introduce the dimensionless variable $\xi = y/\delta$ and argue that the boundary layer's speed $v_x(x, y)$ would be equal to the free stream velocity V times some universal function $f'(\xi)$. This anszatz converted the fluid's partial differential equations into an ordinary differential equation for $f(\xi)$, which we solved numerically.

Our explosion problem is somewhat similar. The characteristic scaling length in the explosion is the radius $R(t)$ of the shock, so the fluid and thermodynamic variables should be expressible as some characteristic values multiplying universal functions of

$$\xi \equiv r/R(t) \, . \tag{16.48}$$

Our thermodynamic variables are P, ρ, u and a natural choice for their characteristic values is the values immediately behind the shock. If we assume that the shock is strong then we can use the strong-shock jump conditions (16.42), (16.43) to determine those values, and

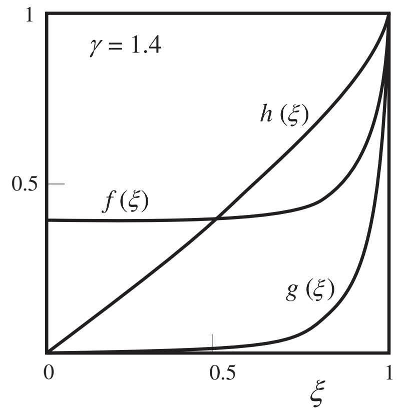

Fig. 16.13: Scaled pressure, density and velocity as a function of scaled radius behind a Sedov-Taylor blast wave in air with $\gamma = 1.4$.

then write

$$
\begin{aligned}
P &= \frac{2}{\gamma+1}\rho_0 \dot{R}^2 f(\xi) \ , \\
\rho &= \frac{\gamma+1}{\gamma-1}\rho_0 g(\xi) \ , \\
v &= \frac{2}{\gamma+1}\dot{R} h(\xi) \ ,
\end{aligned}
\tag{16.49}
$$

with $f(1) = g(1) = h(1) = 1$ since $\xi = 1$ is the shock's location. Note that the velocity v is scaled to the post-shock velocity measured in the inertial frame in which the upstream fluid is at rest, rather than in the non-inertial frame in which the declerating shock is at rest. The self-similarity anszatz (16.49) and resulting self-similar solution for the flow are called the *Sedov-Taylor blast-wave solution*, since L. I. Sedov and G. I. Taylor independently developed it.

We need one more piece of information before we can solve for the flow: the variation of the shock radius R with time. However all that is necessary is the scaling $R = (E/K\rho_0)^{1/5} t^{2/5} \propto t^{2/5}$ [Eq. (16.46)] with the constant K left undetermined for the moment. The partial differential equations (16.47) can then be transformed into ordinary differential equations by inserting the anszatz (16.49), changing the independent variables from r, t to R, ξ, and using

$$
\left(\frac{\partial}{\partial t}\right)_r = -\left(\frac{\xi \dot{R}}{R}\right)\left(\frac{\partial}{\partial \xi}\right)_R + \dot{R}\left(\frac{\partial}{\partial R}\right)_\xi = -\left(\frac{2\xi}{5t}\right)\left(\frac{\partial}{\partial \xi}\right)_R + \frac{2R}{5t}\left(\frac{\partial}{\partial R}\right)_\xi \ , \tag{16.50}
$$

$$
\left(\frac{\partial}{\partial r}\right)_t = \left(\frac{1}{R}\right)\left(\frac{\partial}{\partial \xi}\right)_R \ . \tag{16.51}
$$

The three resulting first order differential equations are rather complex but can in fact be solved analytically (e.g. Landau and Lifshitz 1959). The results for an explosion in air are exhibited in Fig. 16.13.

Armed with these solutions for $f(\xi), g(\xi), h(\xi)$, we can evaluate the flow's energy E, which is equal to the explosion's total energy during the time interval when this similarity solution is accurate. The energy E is given by the integral

$$\begin{aligned} E &= \int_0^R 4\pi r^2 dr \rho \left(\frac{1}{2}v^2 + u\right) \\ &= \frac{4\pi\rho_0 R^3 \dot{R}^2(\gamma+1)}{(\gamma-1)} \int_0^1 d\xi \xi^2 g \left(\frac{2h^2}{(\gamma+1)^2} + \frac{2f}{(\gamma+1)^2 g}\right) . \end{aligned} \tag{16.52}$$

Here we have used Eqs. (16.49) and substituted $u = P/\rho(\gamma-1)$ for the internal energy [Eq. (16.6)]. The energy E appears not only on the left side of this equation, but also on the right, in the terms $\rho_o R^3 \dot{R}^2 = (4/25)E/K$. Thus, E cancels out, and Eq. (16.52) becomes an equation for the unknown constant K. Evaluating that equation numerically, we find that K varies from 2.5 to 1.4 as γ increases from 1.4 (air) to 1.67 (monatomic gas or fully ionised plasma).

It is enlightening to see how the fluid behaves in this blast-wave solution. The fluid that passes through the shock is compressed so that it mostly occupies a fairly thin spherical shell immediately behind the shock [see the spike in $g(\xi)$ in Fig. 16.13]. This shell moves somewhat slower than the shock [$v = 2\dot{R}/(\gamma+1)$; Eq. (16.49) and Fig. 16.13]. As the post-shock flow is subsonic, the pressure within the blast wave is fairly uniform [see the curve $f(\xi)$ in fig. 16.13]; in fact the central pressure is typically half the maximum pressure immediately behind the shock. This pressure pushes on the spherical shell, thereby accelerating the freshly swept-up fluid.

16.6.1 Atomic Bomb

The first atomic bomb was exploded in New Mexico in 1945, and photographs released later that year (Fig. 16.14) showed the radius of the blast wave as a function of time. The pictures were well fit by $R \sim 60(t/1\text{ms})^{0.4}$ m up to about $t = 100$ ms when the shock Mach number fell to about unity (Fig. 16.14). Combining this information with the Sedov-Taylor similarity solution, the Russian physicist L. I. Sedov and others were able to infer the total energy released, which was an official American secret at the time.

If we adopt an intermediate specific heat ratio of $\gamma = 1.5$, as the air will be partially ionised by the shock front, we can use Eq. (16.52) to obtain the estimate $E \sim 1.5 \times 10^{14}$ J or about 20 ktons. (Hydrogen bombs have been manufactured over a thousand times more energetic than the first atomic bombs. However, contemporary arsenals contain bombs that are typically *only* one megaton!)

We can use the Sedov-Taylor solution to infer some further features of the explosion. The post-shock gas is at density $\sim (\gamma+1)/(\gamma-1) \sim 5$ times the ambient density $\rho_0 \sim 1$ kg m^{-3}. Similarly, using the perfect gas law with a mean molecular weight $\mu \sim 10$ and the strong shock jump conditions, the post shock temperature can be computed:

$$T_2 = \frac{m_p \mu}{\rho_2 k} \sim 4 \times 10^4 \left(\frac{t}{1\text{ms}}\right)^{-1.2} \text{K} . \tag{16.53}$$

This is enough to ionise the gas at early times.

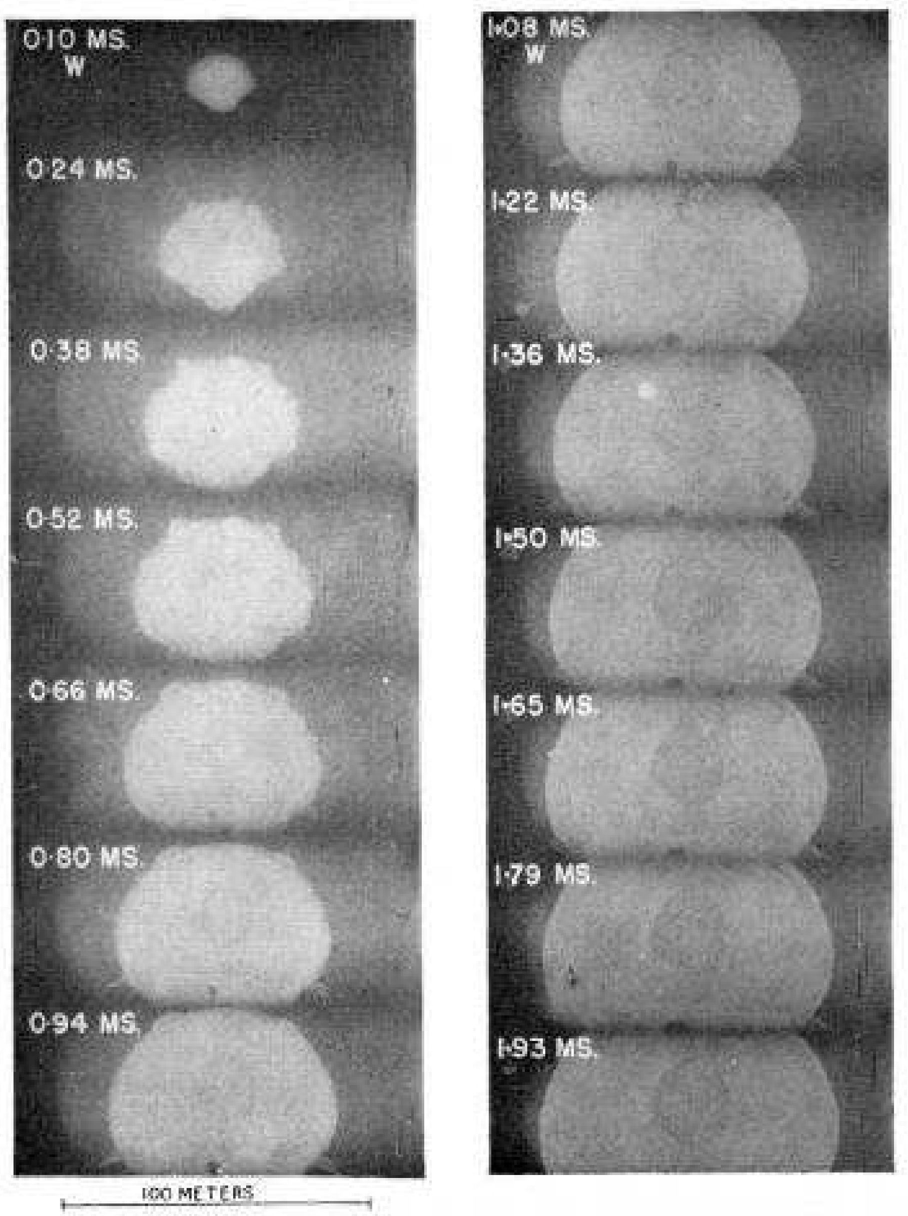

Fig. 16.14: Exploding atomic bomb.

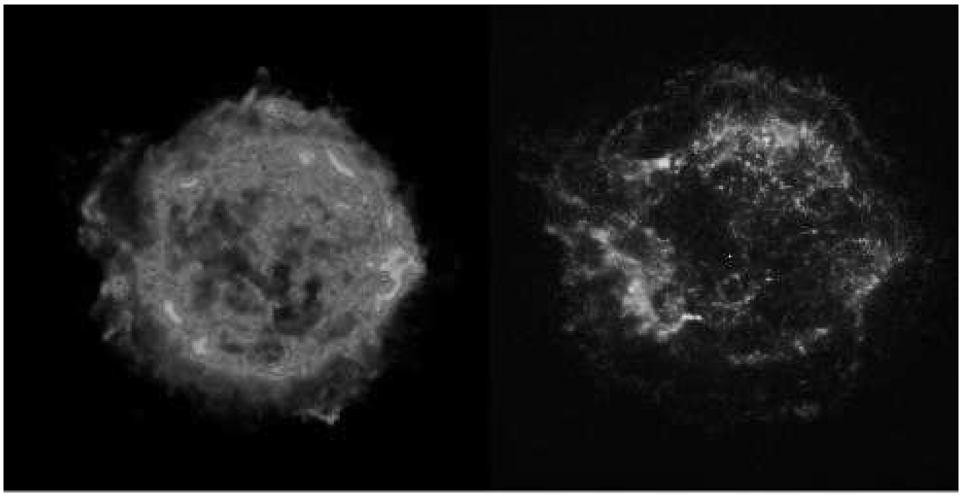

Fig. 16.15: Cassiopeia A – a supernova remnant left behind an exploding star in our galaxy approximately 300 years ago. The image to the left is made using the Very Large Array Radio Telescope; that to the right by the Chandra X-ray Observatory.

16.6.2 Supernovae

The evolution of most massive stars ends in a supernova explosion (like that which was observed in 1987 in the Large Magellanic Cloud), in which a neutron star of mass $m \sim 3 \times 10^{30}$ kg is formed. This neutron star has a gravitational binding energy of about $0.1mc^2 \sim 3 \times 10^{46}$ J. Most of this binding energy is released in the form of neutrinos in the collapse that forms the neutron star, but an energy $E \sim 10^{44}$J drives off the outer envelope of the pre-supernova star, a mass $M_0 \sim 10^{31}$kg. This stellar material escapes with a rms speed $V_0 \sim 2E/M_0{}^{1/2} \sim$ 5000 km s^{-1}. The expanding debris eventually drives a blast wave into the surrounding interstellar medium of density $\rho_0 \sim 10^{-21}$kg m^{-3}. The expansion of the blast wave can be modeled using the Sedov-Taylor solution after the swept-up interstellar gas has become large enough to dominate the blast wave, so the star-dominated initial conditions are no longer important—i.e. after a time $\sim (3M_0/4\pi\rho_0)^{1/3}/V_0 \sim$ 1000yr. The blast wave then decelerates in a Taylor-Sedov self-similar way until the shock speed nears the sound speed in the surrounding gas; this takes about 100,000yr. *Supernova remnants* of this sort are efficient emitters of radio waves and several hundred have been observed in the Galaxy.

In some of the younger examples, like Cassiopeia A, (Fig. 16.15) it is possible to determine the expansion speed, and the effects of deceleration can be measured. The observations are consistent with the prediction of the Sedov-Taylor solution, namely that the radius varries as $R \propto t^{2/5}$, or $\ddot{R} = -3\dot{R}^2/2R$.

****

EXERCISES

Exercise 16.8 *Problem: Underwater explosions*
A simple analytical solution to the Sedov-Taylor similarity equations, can be found for the

particular case $\gamma = 7$. This is a fair approximation to the behavior of water under explosive conditions as it will be almost incompressible.

(i) Make the *ansatz* (whose self-consistency we'll check later), that the velocity in the post-shock flow varies linearly with radius from the origin to the shock, i.e. $h(\xi) = \xi$. Use Eq. (16.50) to transform the equation of continuity into an ordinary differential equation and hence solve for the density function $g(\xi)$.

(ii) Next use the equation of motion to discover that $f(\xi) = \xi^3$.

(iii) Verify that your solutions for the functions f, g, h satisfy the remaining entropy equation therby vindicating the original *ansatz*.

(iv) Finally, substitute into Eq. (16.52) to show that

$$E = \frac{2\pi R^5 \rho_0}{225 t^2}$$

(v) An explosive charge weighing 100kg with an energy release of 10^8J kg^{-1} is detonated underwater. For what range of shock radius do you expect that the Sedov-Taylor similarity solution will be valid?

Exercise 16.9 *Problem: Stellar Winds*
Many stars possess powerful stellar winds which drive strong spherical shock waves into the surrounding interstellar medium. If the strength of the wind remains constant, the kinetic and internal energy of the swept-up interstellar medium will increase linearly with time.

(i) Modify the analysis of the point explosion to show that the speed of the shock wave at time t is $3R(t)/5t$, where R is the associated shock radius. What is the speed of the post-shock gas?

(ii) Now suppose that the star explodes as a supernova and the blast wave expands into the relatively slowly moving stellar wind. Suppose that the rate at which mass has left the star and the speed of the wind have been constant for a long time. How do you expect the density of gas in the wind to vary with radius? Modify the Sedov-Taylor analysis again to show that the expected speed of the shock wave at time t is now $2R(t)/3t$.

****

Bibliography

Landau, L. D. and Lifshitz, E. M. 1959. *Fluid Mechanics*, Reading, Massachusetts: Addison Wesley.

Liepmann, H. & Roshko, A. 1968. *Compressible Gas Dynamics.*

Sedov, L. I. 1959. *Similarity and Dimensional Methods in Mechanics*, New York: Academic Press.

Thompson, P. A. 1984. *Compressible Fluid Dynamics*, Maple Press Co.

Van Dyke, M. 1982. *An Album of Fluid Flow*, Stanford: Parabolic Press.

Zeldovich, Ya. B. & Raizer, Yu. P. 1979. *Physics of Shock Waves and High Temperature Hydrodynamic Phenomena.*